Title: Loss of brain insulin production impairs learning and memory in female mice

Authors: Stella Baehring[1#], Timothy P. O'Leary[1#], Haoning Howard Cen, Danae Holenka[1], Kyungchan Kim[2], Sunday Ajayi, Daniel Semenov[1], Manuel Belmadani[3], Hong Li[1], Arya E. Mehran[1], Honey Modi[1], Melissa M. Page[1], Søs Skovsø[4], Paul Pavlidis[3], Shernaz X. Bamji[1], Eun-Kyoung Kim[2], James D. Johnson[1*]

Affiliations:
[1] Life Sciences Institute, Department of Cellular and Physiological Sciences & Department of Surgery, University of British Columbia, Vancouver, Canada
[2] Department of Brain and Cognitive Sciences and Neurometabolomics Research Center, Daegu Gyeongbuk Institute of Science and Technology, Daegu, Republic of Korea
[3] Michael Smith Laboratories, University of British Columbia, Vancouver, Canada
[4] Valkyrie Life Sciences, Vancouver, Canada

[#] These authors contributed equally.

***Address correspondence to:** James D. Johnson, PhD., Faculty of Medicine, Department Cellular and Physiological Sciences, The University of British Columbia, Life Sciences Institute, 5358 – 2350 Health Sciences Mall, Vancouver, British Columbia, Canada V6T 1Z3
Phone: 604 822 7187, Email: James.d.johnson@ubc.ca, Bluesky: @JimJohnsonSci

Abstract word count: 273
Word count: 10,268
Reference count: 66
Figure count: 6
Supplemental figure count: 1

Keywords: Central insulin production; learning and memory; Alzheimer's disease; hippocampus
Declaration of Interests: The authors declare no competing interests.
Funding: Work was supported by a Brain Canada Multi-Investigator grant to J.D.J., S.X.B., and P.P.
Acknowledgments: We thank many colleagues for helpful discussions.
Data availability: RNA sequencing data are online. All other data are available on request.

Author Contributions:
S.B. designed studies, performed experiments, analyzed/interpreted data, and co-wrote the manuscript.
T.O. designed studies, performed experiments, analyzed/interpreted data, and co-wrote the manuscript.
H.H.C. analyzed bioinformatic data and helped write the manuscript.
D.H. performed experiments, analyzed/interpreted data.
K.K. performed experiments.
S.A. performed experiments.
D.S. performed experiments.
M.B. performed experiments and analyzed bioinformatic data.
H.L. performed experiments.
A.E.M. performed experiments, analyzed/interpreted data.
H.M. performed experiments, analyzed/interpreted data.
M.M.P. performed experiments, analyzed/interpreted data
S.S. performed experiments, analyzed/interpreted data.
P.P. supported bioinformatic studies, interpreted data, and edited the manuscript
S.X.B. designed studies, interpreted data, and edited the manuscript
E-K. K. analyzed data and provided a key reagent.
J.D.J. conceived the project, designed studies, interpreted data, co-wrote the manuscript, and is the guarantor of this work.

Abstract

Diabetes is a metabolic disorder characterized by dysfunctional insulin release and action, and it is a risk factor for Alzheimer's disease, the most common form of dementia. Alterations in brain insulin signalling and metabolism have been linked with Alzheimer's disease in multiple studies. It has been previously shown that the ancestral insulin gene, *Ins2*, is transcribed locally within the brain. Here we demonstrate that *Ins2* mRNA is higher in females than males, and modulated by diet. Moreover, we demonstrate that the Ins2 protein is found in the hippocampus, a brain region with established roles in learning and memory. To specifically determine how insulin produced locally in the brain influences hippocampal function, specifically learning and memory, we used mice with germline *Ins2* knockout (*Ins2*$^{-/-}$) and the normal complement of wildtype *Ins1* alleles. Compensation from the *Ins1* gene ensured normal glucose tolerance, normal insulin sensitivity, normal fasting insulin, and normal body weight under these conditions. We assessed visuo-spatial learning and memory in male and female *Ins2*$^{-/-}$ and wild-type littermate control mice using the Morris water maze (MWM). Learning and memory performance of female *Ins2*$^{-/-}$ mice was significantly impaired relative to wild-type mice, whereas the performance of male *Ins2*$^{-/-}$ and wild-type mice did not differ. We profiled isolated hippocampi from female *Ins2*$^{-/-}$ and littermate control mice using RNA sequencing to provide an unbiased analysis of gene expression differences that underlie these behavioural changes. Cyclin D1 (*Ccnd1*) was significantly reduced in *Ins2*$^{-/-}$ mice, prompting us to examine adult neurogenesis using exogenous mitotic marker EdU and the immature neuronal marker doublecortin (DCX). Collectively, our data demonstrate female-specific role for brain-derived *Ins2* on learning and memory function in mice.

Introduction

Diabetes is a significant risk factor for dementia (1) and people with type 2 diabetes can present with cognitive impairment, specifically in learning and memory, similarly to early onset Alzheimer's disease (2). People with Alzheimer's disease often present with hyperglycemia and insulin dysfunction in peripheral organs, and may also have 'insulin resistance' in the brain (3). Post-mortem brain tissue pointed to impaired insulin signalling in the cerebral cortex and hippocampus of Alzheimer's disease samples compared to control (4). Studies in humans and animals show that insulin plays a multifactorial role in brain function such as enhancing synaptic plasticity, dendritic spine formation, and increasing neurotransmitter turnover (5, 6). Insulin also influences the clearance of the amyloid β peptide and phosphorylation of tau, which are hallmarks of Alzheimer's Disease (7). Insulin insensitivity in the brain is associated with reduced insulin receptor levels, binding affinity, and disrupts insulin signalling (8). Insulin signalling is altered in the brains of Alzheimer's disease patients and alterations in insulin receptor substrates (IRS-1 and IRS-2) is an early pathological characteristic (9). A recent study found that the loss of insulin signaling in astrocytes exacerbates Alzheimer-like phenotypes including amyloid plaque accumulation (10). Astrocytes are crucial in regulating important neuronal functions via insulin, such as dopaminergic signaling and cholesterol synthesis, pointing to the importance of insulin availability in local brain regions (11). Interestingly, insulin in the brain is produced by neurons, but not glial cells (12, 13). Together, these separate lines of evidence suggest that impairment of brain insulin action may underly a component of the pathology of Alzheimer's disease. Since insulin action on the brain plays a significant role in cognitive functions in humans and various pre-clinical model systems (14-16), some have proposed administering insulin directly to the brain as a treatment bypassing metabolic and brain barriers that decrease bioavailability (17). Indeed, augmenting insulin signalling tone via intranasal administration of insulin can improve cognitive function in Alzheimer's disease patients (14, 17). Lifestyle interventions that increase insulin sensitivity, such as diet and exercise, improve learning and memory, and are being used as preventative and therapeutic approaches for Alzheimer's disease (6, 18, 19). Collectively evidence points to a potential role for brain-directed insulin and insulin signalling on cognition.

Most studies investigating the effects of insulin on the brain were done under the assumption that insulin in the brain is of pancreatic origin. Although peripheral insulin crosses the blood brain barrier via receptor-mediated transport (20), accumulating evidence shows that insulin is also produced locally in the brain (21). Insulin expression has been measured in several brain regions, including cerebral cortex,

choroid plexus, cerebellum, and the hippocampus (22-27). The hippocampus is also the main region involved in memory and learning, as well as the first to be affected by neural deterioration in Alzheimer's disease. In mice, the specificity of these observations has been confirmed with mice lacking insulin 2 (*Ins2*) gene (human homolog)(25, 26), which live due to the presence of an additional, pancreas-specific insulin coding gene insulin 1 (*Ins1*)(28). Notably, we have previously shown that *Ins1* does not upregulate its gene expression in the brain to compensate for *Ins2* loss (25, 26). Insulin synthesis has been reported in neuronal progenitors of the hippocampus and olfactory bulbs (12, 23), key sites of adulthood neurogenesis (29, 30). Studies on neurogenesis showed that activation of insulin in the neurogenic niche stimulates neural stem cell survival, proliferation, and differentiation (31, 32), suggesting that brain insulin and neurogenesis could be linked. Collectively, these data and others (25, 26) clearly demonstrate that a small amount of insulin can be synthesized in the brain and that its production occurs in regions highly relevant for learning and memory. However, little is known about the environmental factors that influence insulin production in the brain. Most importantly, whether brain-derived insulin directly influences learning, memory, and neurogenesis has yet to be examined.

In this study, we used *Ins2* knockout mice to further confirm protein insulin synthesis in the hippocampus and tested how the loss of *Ins2* influences learning and memory in both sexes. We determined that *Ins2* expression in the mouse hippocampus is modulated by diet and biological sex. We found that female mice lacking *Ins2* have deficits in learning and memory. These data provide the first loss-of-function evidence that *Ins2* plays a role in hippocampus-controlled behaviour.

Materials and Methods

Experimental animals

Experiments charactering *Ins2* expression used five-month-old C57BL/6J mice (Strain 000664). All other experiments used male and female *Ins2*$^{+/+}$ (wild-type) and *Ins2*$^{-/-}$ (knockout) littermates between 3-18 months of age. *Ins2*$^{-/-}$ mice were originally made by Duville et al (33) and have the LacZ/neomycin cassette inserted into the *Ins2* locus. Mice were bred in-house, by crossing male and female *Ins2*$^{+/-}$ mice. Mice were housed in same-sex groups of 2-4, in cages with a plastic dome and nesting material for enrichment. In some cases, mice were singly housed due to aggression or barbering, but effort was taken to ensure a similar number of singly housed mice were present for each genotype and sex. Except where indicated, food and water were available *ad libitum*. Mice received a chow diet (total calories = 4.68 kcal/g; 25.3% calories from fat, 19.8% calories from protein, 54.9% calories from carbohydrate; Catalog #5015 Lab Diets, Richmond, IN) or a high fat diet (total calories = 5.56 kcal/g; 58.0% calories from fat, 16.4% calories from protein, 25.5% calories from carbohydrate; Catalog #D12330 Open-Source Diets/Research Diets, New Brunswick, NJ). Mice were housed on a reverse 12 h light dark cycle (lights off at 7:00 am), and all experiments were completed during the dark phase of the light cycle. Transport of mice from the home-cage to behavioral tests was completed with a 500 ml plastic container to reduce handling stress. Some studies used mice with GFP knocked into the endogenous *Ins2* gene locus, which have been described and phenotyped elsewhere (34). All experimental procedures were approved by the UBC animal care committee and adhered to Canadian Council on Animal Care guidelines.

Immunohistochemistry and immunoblotting for C peptide, β-gal and pro-insulin

Mice were perfused under isoflurane anesthesia with phosphate-buffered saline (PBS), followed by ice-cold 4% paraformaldehyde in PBS. Brains were post-fixed in paraformaldehyde for 4 hrs, and then cryoprotected with 30% sucrose in PBS for 48 hours. Brains were embedded in OCT, frozen on dry-ice and stored at -80ºC, before sectioning at 40µm on a cryostat. Immunostaining was completed using rabbit anti–C-peptide (1:300; Cell Signaling Technology, 4593), rabbit anti–β-gal (1:100; Thermo Fisher Scientific, A-11132) and mouse anti-proinsulin (1:100; R&D Systems, Bio-Techne, MAB13361) primary anti-bodies. The Donkey anti-rabbit Cy3 (1:200; Jackson ImmunoResearch, 711-165-152) and Donkey anti-mouse Alexa488 (1:200; Jackson ImmunoResearch, 715-545-150) were used as secondary antibodies, followed by nuclear staining with Hoechst 33258 (1ug/ml, Invitrogen, Thermo Fisher

Scientific). Sections were mounted onto slides, cover-slipped with VECTASHIELD mounting medium (Vector Laboratories), and imaged using a LSM 800 confocal microscope (Carl Zeiss).

Immunoblots of proinsulin was conducted as in our previous publication (26). Briefly, mice were perfused with 10 mL of ice-cold phosphate-buffered saline before collecting the samples. To extract protein from the pancreas and hippocampus, samples were dissolved in lysis buffers as described previously (26, 35). The total hippocampus of 5 *Ins2*$^{+/+}$ and 5 *Ins2*$^{-/-}$ mice were lysed and separated on 15% SDS-PAGE and blotted onto polyvinylidene difluoride membranes (Millipore, IPVH00010) for 30 minutes at 16 V in the transfer buffer (25 mM Tris base, pH 7.4, 192 mM glycine, 10% methanol). The membranes were blocked with 5% skim milk for 1 hour and then incubated with primary antibody against proinsulin (1:1000; Cell Signaling Technology, 8138) or GAPDH (1:10,000; Cell Signaling Technology, 2118) at 4°C overnight. After extensive washing in Tris-buffered saline with 0.1% Tween-20, the membranes were incubated with horseradish peroxidase-conjugated anti-mouse (1:3000; Cell Signaling Technology, 7076S) or anti-rabbit secondary antibody (1:10,000; Thermo Scientific, NCI1460KR) and the bands were visualized using ECL solutions (Thermo Scientific, NCI4080KR; Advansta, K-12045-D50) according to the manufacturer's instructions.

RNA extraction, cDNA synthesis and quantitative polymerase chain reaction

Brains were rapidly removed from mice following decapitation after C02 euthanasia. Dissection of the brain occurred on ice, wherein the hippocampus, cerebellum, cerebral cortex, olfactory bulbs, hypothalamus and midbrain (including all residual tissue) were isolated. All brain tissue was then snap frozen on dry ice and stored at -80°C. Animals were euthanized in an alternating sequence based on sex to mitigate circadian effects on gene transcription. Dissected brain tissue was homogenized in Trizol (Thermo Fisher) to protect against RNA degradation. Chloroform (50ul) was then added, and the tissue and shaken for 20 seconds before a 15-minute incubation at room temperature. Samples were centrifuged (14000rpm, 15 minutes at 4°C) and the aqueous phase was transferred to 70% ethanol. RNA extraction was performed using the Qiagen RNasy minikit (cat #74108 Thermo Fisher), while DNA was synthesized using the qScript cDNA Synthesis Kit (cat#101414-100, Quanta Bioscience).

Ins2 mRNA was measured using quantitative polymerase chain reaction (qPCR). The cDNA was subjected to Taqman real-time PCR (StepOnePlus, Applied Biosystems). The following primers were used; *Ins2* Taqman reverse 280→259: GAT CTA CAA TGC CAC GCT TCT G, *Ins2* Taqman probe 224→207: CCT GCT CCC GGG CCT CCA. PCR conditions were 2 min at 50°C, 10 min at 95°C and 40 cycles 15-sec cycles at 95°C and lastly 1 min at 60°C. Samples were normalized to the housekeeping gene beta actin by converting raw values to delta values. Reverse log of delta values were used for all analyses. Water and *Ins2*$^{-/-}$ tissue were used as negative controls in all experiments.

Metabolic characterization

Age-related metabolic phenotyping included measurement of body weight, fasting blood glucose (FBG), glucose tolerance tests (GTT), insulin tolerance tests (ITT) and glucose stimulated insulin secretion (GSIS). For FBG and GTT, mice were fasted for four hours in clean cages prior to glucose measurement. For GTT and ITT, baseline levels of glucose were obtained 15 min prior to intra-peritoneal injections of either glucose (GTT; 4mg/kg) or insulin (ITT; 0.75U/kg, or 1.5U/kg) in PBS. Blood glucose was then measured at 15, 30, 60, 90 and 120 min after injections using OneTouch glucometers and measurement strips. For GSIS, the legs of mice were shaved to facilitate blood collection from the lateral saphenous vein. Mice were fasted for 4 hours, and baseline blood samples were obtained, followed an intra-peritoneal injection of glucose (4mg/kg). Blood samples were then obtained at 15 and 30min post injection. All blood samples were kept on ice, before being centrifuged and serum collected. Insulin levels were then quantified using an enzyme linked immunosorbent assay, based on the manufacturer's instructions (ALPCO Diagnostics, Salem, NH).

Morris water maze

The Morris water maze consisted of a white circular pool (110 cm diameter) filled with water to a depth of 16 cm. The water was 23°C and made opaque with the addition of non-toxic white tempera paint (Schola, 2002737). A circular escape platform (11.5 cm diameter) was placed in the pool and was

0.5cm below the water surface. The water maze was placed in a diffusely lit room with many extra-maze cues, including large geometric posters adhered to the walls, a desk with a computer, a door, and the geometric layout of the room. The experimenter also served as an extra-maze cue and stood in a similar position for each trial. Mice were placed individually into holding cages lined with paper towel during training. The Anymaze computer tracking system was used to record the movement of mice, and to obtain measures of learning and memory performance.

Mice first completed acquisition training consisted of 6 days of training with 4 trials per day. The escape platform was located in the same location (NW quadrant) across trials. For each trial, mice were placed into the pool at one of four release locations (pseudo-randomly determined) and were given a maximum of 60 sec to reach the escape platform. After reaching the platform, mice remained on the platform for 5-10 seconds before being returned to the holding cage. If mice did not reach the platform in 60 sec, they were guided to the platform by the experimenter. Mice were tested in squads of 4-6, and the inter-trial interval ranged from 2-8 minutes. Performance of mice was measured using latency to locate the escape platform, distance travelled to reach the escape platform, cumulative search error and swim-speed. Cumulative search error was obtained using custom software and consisted of the total distance from the escape platform, summed across all recorded positions of the mouse (5 hz). A correction factor is applied, where the CSE value expected for the optimal swim path (determined by start location and swim speed) is subtracted from the total CSE.

The day following acquisition training, mice completed a 60 sec probe trial without the escape platform to measure memory. The number of times mice crossed over the location of the escape platform (annulus crossings) and respective locations in other quadrants of the pool were recorded. The day following the acquisition probe, mice completed an additional day of training (acquisition re-training) to determine the extent of extinction occurred in the probe trial, and to re-establish baseline levels of learning performance.

Mice then completed reversal training to measure behavioral flexibility and learning a new spatial location of the escape platform. During reversal training the escape platform was moved to the opposite side of the pool. Mice completed 6 days of training with 4 trials per day, using the same procedure as acquisition training. Following reversal training, mice completed a 60-sec probe trial to measure memory for the new escape platform location.

Anxiety-like behaviour

Mice were tested on the open-field, light-dark box and elevated plus maze to measure locomotor activity and anxiety-like behaviour. All trials were 10 min in length and the test apparatuses were cleaned with 70% ethanol between trials. After trials, mice were placed in a clean holding cage, while the remaining cage-mates completed their trials. During testing mice were brought in groups of 7-9 mice into a dark and quiet anteroom. Mice habituated to the anteroom for at least 25 min before behavioral testing. Testing was completed in a different room than Morris water maze training. Tests were completed with 7-13- day intervals, to reduce potential cross-test habituation. Movement of mice in the open-field, light-dark box and elevated plus maze were recorded with the Ethovision (Noldus) video tracking system. Species typical behaviors were measured with the Boris (Friad and Gamba, 2016) event scoring software, using video recordings from trials.

The open field consisted of a box (70 x 70 cm) made of transparent Plexiglas, with 23 cm high walls. For each trial, mice were placed into the one of four corners of the open field (pseudo-randomly determined). Locomotor activity was measured with distance travelled, while anxiety-like behaviour was assessed with entries into the center of the open-field (9th of area). Species typical behaviors were also recorded including number of rears, grooming duration, and freezing duration.

The light-dark box was constructed from Plexiglas and was divided into two chambers that were either brightly (light zone) or dimly lit (dark zone). A single light placed above the light zone provided lighting in the light-dark box and testing room. For each trial, mice were placed in the light zone facing the opening to the dark zone. The same behavioural measures recorded in the OF were also recorded in the light-dark box, except that time in the light chamber was used as a measure of anxiety-like behaviour.

The elevated plus maze consisted of two pairs of arms, each attached to a central square. One pair of arms had opaque walls around the edge (closed arms), while the other pair of arms had no walls (open arms). A small rim (0.5 cm) was present around the edge of the open arms to prevent mice from falling. A single light provided dim lighting for the elevated plus maze and testing room. For each trial, mice were placed onto the central hub of the elevated plus maze, facing a closed arm. The same behavioral measures recorded in the open-field were also recorded in the elevated plus maze, except that time in the open arms was used as measure of anxiety-like behavour. The number of times mice dipped their heads over the edge of the open arms (head-dips) was also recorded as a species typical measure of anxiety-like behaviour.

Bulk hippocampal RNA sequencing

Removal and dissection of brains were completed as described above for qPCR. Animals were euthanized in an alternating sequence based on genotype to prevent potential circadian effects on gene transcription. Body weight and un-fasted blood glucose (measured the from neck after decapitation) were also measured to ensure no pre-existing differences between *Ins2*$^{+/+}$ and *Ins2*$^{-/-}$ mice at the time of euthanasia. Sample quality control was performed using the Agilent 2100 Bioanalyzer. Qualifying samples were then prepped following the standard protocol for the NEBnext Ultra ii Stranded mRNA (New England Biolabs). Sequencing was performed on the Illumina NextSeq 500 with Paired End 43bp × 43bp reads. Sequencing data was demultiplexed using Illumina's bcl2fastq2. De-multiplexed read sequences were then aligned to the Mus Musculous (PAR-masked)/mm10 reference sequence using STAR aligner. Quality control led to one outlier sample (genotype -/-) being removed. Hierarchical clustering and principal component analysis (PCA) identified 3 additional outliers (1 *Ins2*$^{+/+}$ and 2 *Ins2*) that were removed. Genes with expression below 0.5 counts per million were dropped from the analysis. Differential expression analysis associated with genotype was performed using limma-trend (36) after quantile normalization or using DESeq2 (37), which had consistent results. The DESeq2 results were used in the figures and Gene Set Enrichment Analysis (GSEA). GSEA was performed with clusterProfiler R package using Gene Ontology (Biological Process) knowledgebase (FDR < 0.0001) (38), and simplify() function was used to remove redundant GO terms (https://guangchuangyu.github.io/2015/10/use-simplify-to-remove-redundancy-of-enriched-go-terms/).

Quantification of adult hipppcampal neurogenesis

Twenty-month-old *Ins2*$^{+/+}$ and *Ins2*$^{-/-}$ mice were given EdU in drinking water (0.25 mg/ml) for four weeks. The EdU water was freshly prepared every week and was given to mice in 120 ml bottles. Body weight and water consumption were recorded every week to ensure consumption of EdU water. Mice with given Edu-water for 4 weeks, after which they were transcardially perfused with PBS (0.1M) followed by 4% paraformaldehyde. Brains were extracted, post-fixed in 4% paraformaldehyde overnight, and then transferred to a 30% sucrose solution for cryoprotection. Brains were sliced into 40 µm coronal sections using a cryostat at -20°C. Sections were collected in series of 6 through the rostral-caudal extent of the hippocampus and stored in anti-freeze solution (ethylene glycol, glycerol, and 0.1 M PBS) at -20°C until immunostaining.

To measure adult neurogenesis a series of sections were stained for both EdU and doublecortin (DCX). Staining for EdU was completed with the Click-iT Plus EdU Alexa Fluor 647 Imaging Kit (Thermo Fisher Scientific). Staining for DCX was completed via Immunohistochemistry using a Rabbit anti-DCX IgG polyclonal antibody (cat# 326 003 Thermo Scientific) and a Donkey anti-Rabbit IgG H+L Alexa Fluor 488 secondary antibody (cat# A-21206 Invitrogen). We used vertical sections of intestinal villi from EdU treated animals as positive controls for EdU labelling.

Stained sections were imaged with a Zeiss LSM 880 confocal microscope. Dorsal and ventral regions of the dentate gyrus were imaged using a 20X objective. Image stacks trough the section were obtained, stitched together and maximum intensity projections were then used to count EdU and DCX-positive cells. The experimenter was blind to all conditions during quantification, and six sections were analyzed per animal. The sampling area within the dentate gyrus was also obtained, and cell counts normalized to sampling area.

Statistical Analysis

For data using WT C57BL/6J mice, data was analyzed with sex as a factor when possible. Subsequent data for experiments using *Ins2*$^{+/+}$ and *Ins2*$^{-/-}$ mice were analyzed separately for each sex and age to increase statistical power to detect differences due to genotype. For tolerance tests and glucose stimulated insulin secretion, mixed design ANOVAs (2 x 6 or 2 x 3, respectively) were used with genotype as a between subject factor and sampling time as a within subject factor. For acquisition and reversal training in the MWM, analyses were completed separately for days 1-3 and days 4-6, which reflect initial learning and near-asymptotic performance respectively. Measures of learning performance were analyzed with mixed design ANOVAs (2 x 3), using genotype as a between subject factor and day of training as within subject factor. All other analyses were completed using one-way between subject ANOVAs comparing genotypes. Post-hoc tests were completed using unpaired t-tests, with Bonferonni corrections applied independently for each statistical test.

Results

Ins2 is produced in the brain and its expression is sexually dimorphic and modulated by diet

We previously identified *Ins2* mRNA and insulin protein in the mouse brain (25), but did not show hippocampal C-peptide and proinsulin immunoreactivity that was specific (i.e. absent in *Ins2* null brains). Here, we showed that labelling of C-peptide, a byproduct and marker of insulin synthesis, can be observed within the hippocampus of *Ins2*$^{+/+}$ mice, particularly within the dentate gyrus-CA3 pathway (**Figure 1A)**. This was confirmed with immunoblots showing a small but clear *Ins2*-specific band for proinsulin in hippocampus lysates, as well as the expected prominent band in pancreas (**Figure 1B**). As expected, no insulin protein was found in hippocampi from *Ins2*$^{-/-}$ because the non-ancestral *Ins1* gene is not robustly expressed in the mouse brain (25). Complementary immunostaining in the hippocampus of wildtype *Ins2*$^{+/+}$ mice revealed clear labelling of proinsulin within the CA3 and choroid plexus, and this staining was largely absent in *Ins2*$^{-/-}$ mice (**Figure 1C**). Importantly, in *Ins2*$^{+/-}$ mice, proinsulin labelling colocalized with β-gal labelling, a proxy for *Ins2* gene activity and mRNA expression. We were also able to visualize green fluorescence in cultured hippocampal neurons from mice with GFP knocked into the endogenous *Ins2* locus, which we have previously shown correlates with *Ins2* mRNA, pre-mRNA, and proteins levels (34) (**Figure 1D**). Together, these data provide further strong evidence that the brain can locally produce insulin.

We next measured *Ins2* mRNA levels across six brain regions (hippocampus, cerebellum, cerebral cortex, olfactory bulbs, hypothalamus, all residual tissue was classified as midbrain) in male and female C57BL/6J mice. *Ins2* expression was highest in the hippocampus and cerebellum of both sexes (**Figure 2A**). *Ins2* mRNA was consistently higher in females than males ($F(1,14) = 7.58$, $p < 0.05$), and clear differences were observed across brain regions ($F(5,70) = 18.42$, $p < 0.0001$). Sex differences in *Ins2* expression were more prominent within certain brain regions (interaction, ($F(5,70) = 2.67$, $p < 0.05$)), where females showed higher expression of *Ins2* than males in the hippocampus and cerebellum (post-hoc, $p < 0.005$) (**Figure 2A**). Because the expression of *Ins2* and levels of insulin in the pancreas are modulated by diet, so we next tested whether a similar regulation occurs in brain. These independent experiments confirmed higher expression of *Ins2* in the hippocampus of female mice relative to other brain regions (i.e. cerebral cortex) and relative to males **(Figure 2B,C)**. In female mice, *Ins2* expression was reduced after being fed a high-fat diet when compared to a control diet, whereas diet did not affect *Ins2* expression in male mice (**Figure 2B,C**). These data demonstrate that *Ins2* mRNA levels differ between brain regions, sexes, and dietary contexts.

Ins1 is sufficient to preserve normal peripheral metabolism in the absence of Ins2

Before using *Ins2*$^{-/-}$ mice to examine the physiological roles of Ins2 in the brain, it was critical to confirm that this was independent of significant whole-body metabolic effects. Previous studies have shown that mice lacking *Ins2* alone for life have relatively normal metabolic physiology (25), supporting previous observations that *Ins1* can compensate for loss of *Ins2* (39). Previous work only focused on males, so we next characterized metabolism in littermate male and female *Ins2*$^{-/-}$ mice side-by-side to confirm that *Ins1* can compensate for loss of *Ins2 in* both sexes. In addition, we examined mice from 3-

16 months of age to determine if compensation by *Ins1* can be maintained during aging. For both males and females, body weight of *Ins2*$^{-/-}$ mice did not differ from *Ins2*$^{+/+}$ mice at any age **(Figure 3A,B)**. Fasted (4 hours) blood glucose levels were largely similar between *Ins2*$^{-/-}$ and *Ins2*$^{+/+}$ mice and differed only in males at the oldest age (16-18 months) tested (**Figure 3C,D)**. *Ins2*$^{-/-}$ and *Ins2*$^{+/+}$ mice did not differ in glucose tolerance tests **(Figure 3E-H)** nor in insulin tolerance tests at either 8 or 16-18 months of age **(Figure 3I-L)**. *Ins2*$^{-/-}$ and *Ins2*$^{+/+}$ mice also showed similar glucose stimulated insulin secretion (**Figure 3M-P**), although there was a trend for higher insulin in female *Ins2*$^{+/+}$ mice compared with *Ins2*$^{-/-}$ mice at the oldest age measured (**Figure 3N**). Together, these data suggest that *Ins1* can produce a near-complete compensation for the absence of *Ins2* in both male and female mice on this normal chow diet, and this compensation can be maintained through aging up to 16-18 months.

Loss of Ins2 produces visuo-spatial learning and memory impairments in female, but not male mice

The hippocampus is critical for a variety of different cognitive processes, and in rodents is perhaps most well-known for its role in visuo-spatial navigation and memory (40). Given *Ins2* expression is prominent within the hippocampus relative to other neuronal populations, we next examined whether hippocampal-dependent behaviour was affected by *Ins2*$^{-/-}$ ablation in the Morris water maze, a commonly used and well-validated test of visuo-spatial learning and memory in rodents (41). Given that the sexual dimorphism in hippocampal *Ins2* expression, we compared aged female (**Figure 4A-F**) and male (**Figure 4G-L**) littermates of both genotypes.

During acquisition training, female *Ins2*$^{-/-}$ and *Ins2*$^{+/+}$ mice did not differ on measures of learning including latency (**Figure 4A**), distance (**Figure 4D**), or cumulative search error (**Figure 4B**). During the acquisition probe memory test, however, female *Ins2*$^{-/-}$ completed fewer crossings over the location of the escape platform (annulus crossings) than *Ins2*$^{+/+}$ mice **(Figure 4C)**. We then provided an additional day of acquisition training (re-training, RT) to reduce potential extinction effects, and to provide an additional indirect measure of memory by assessing retention of learning performance from the last day of acquisition training (2 days prior). On the re-training day, female *Ins2*$^{-/-}$ performed worse than *Ins2*$^{+/+}$, mice on all measures of learning performance (**Figure 4A,B,D**). During first 3 days of reversal training, female *Ins2*$^{-/-}$ and *Ins2*$^{+/+}$ did not differ on measures of learning performance; over the last 3 days of reversal training, however, female *Ins2*$^{-/-}$ mice performed worse than *Ins2*$^{+/+}$ mice on all measures of learning performance (**Figure 4A,B,D**). During the reversal probe memory test, *Ins2*$^{-/-}$ mice completed fewer crossings over the escape platform location than *Ins2*$^{+/+}$ mice **(Figure 4D)**. We also measured swim speed of mice throughout acquisition and reversal training, which can reflect motivation to find the escape platform. Although, female *Ins2*$^{-/-}$ mice swam quicker than *Ins2*$^{+/+}$ mice during the first 3 days of acquisition training, this difference was not present during the last 3 days of acquisition training, or at any point during reversal training **(Figure 4E)**. Given that differences in learning performance were not present in acquisition training, we can conclude that differences in swim-speed do not account for the impaired learning and memory observed in *Ins2*$^{-/-}$ mice. Taken together, these results indicate impaired learning and memory for the reversal escape platform location in *Ins2*$^{-/-}$ mice.

We also assessed learning and memory in male *Ins2*$^{-/-}$ and *Ins2*$^{+/+}$ mice in the Morris water maze but did not find any differences in learning performance during either acquisition or reversal training **(Figure 4G,H,J,K).** We also did not observe differences in memory performance during acquisition or reversal memory probe tests **(Figure 4I,L)**. Thus, unlike female mice, loss of *Ins2*$^{-/-}$ in male mice is not sufficient to disrupt visuo-spatial learning or memory.

Loss of Ins2 does not influence anxiety-like behaviour or locomotor activity.

The function of the hippocampus is known to differ along its dorsal-ventral axis, with the dorsal hippocampus being involved in visuo-spatial navigation and memory, and the ventral hippocampus being involved more so in anxiety-related behaviour (42, 43). Therefore, we examined anxiety-like behaviour in *Ins2*$^{-/-}$ mice, to provide a more complete picture for the role of *Ins2* on hippocampal function. *Ins2*$^{-/-}$ and *Ins2*$^{+/+}$ mice were tested on three commonly used tests of anxiety-like behaviour: the open-field, light-dark box, and elevated-plus maze. All three tests were effective in producing marked avoidance of anxiogenic areas, with mice spending less time in anxiogenic regions than expected by

chance **(Supplemental Figure 1)**. For both males and females, however, *Ins2*$^{-/-}$ and *Ins2*$^{+/+}$ mice did not differ in anxiety-related behaviour on the OF, LDB or EPM. We also extended our analysis to include species-typical measures of exploration and anxiety-like behaviour (i.e. grooming, rearing, freezing, etc.), but did not find any differences between *Ins2*$^{-/-}$ and *Ins2*$^{+/+}$ mice **(Supplemental Figure 1)**. Each of the OF, LDB and EPM can also be used to assess locomotor activity within novel environments, however, we did not observe any differences between *Ins2*$^{-/-}$ and *Ins2*$^{+/+}$ mice in locomotor activity in either males or females **(Supplemental Figure 1)**. Thus, the effects of *Ins2* knockout in female mice appear to be specific to learning and memory in the Morris water maze.

Transcriptomics of hippocampi from aged female Ins2$^{-/-}$ *mice identifies cyclin D1 as downregulated*

We conducted bulk hippocampal RNA-seq in aged female *Ins2*$^{-/-}$ mice to identify potential molecular mechanisms that could underlie the defects in learning and memory. We started with 11 samples in each group, but three samples were deemed outliers based on hierarchical clustering and PCA and were removed from the analysis (**Figure 6A,B**). We confirmed the absence of *Ins2* mRNA in female *Ins2*$^{-/-}$ mice **(Figure 6C**). Then, we identified 6 downregulated and 13 upregulated genes in *Ins2*$^{-/-}$ *mice* (**Figure 6D**). Among them, the cell cycle regulatory gene *Ccnd1* and the stem cell regulatory long non-coding RNA Gm26793 (44) were the most significantly downregulated and upregulated genes, respectively. It should be noted that these genes were robustly altered even when the outlier samples were included. Gene set enrichment analysis showed that the (semi-redundant) gene ontology terms “aerobic respiration” and “oxidative phosphorylation” were the most significantly upregulated pathways (**Figure 6E**). Insulin is known to be a regulator of oxidative phosphorylation in many tissues, including the brain (45). The gene ontology term “epithelium development” was the only significantly downregulated pathway (**Figure 6E**). Together, these relatively well-powered transcriptomic studies point to potential molecular mechanisms underlying the effects of insulin signalling the in female rodent hippocampus.

Neurogenesis in Ins2$^{-/-}$ *mice.*

Given that *Ins2*$^{-/-}$ mice had reduced *Ccnd1* mRNA, a gene with known roles in neurogenesis, we next examined if hippocampal neurogenesis was altered in aged *Ins2*$^{-/-}$ mice using EdU, a thymidine analogue that incorporates into proliferating cells, and by identifying immature neurons via doublecortin. We first confirmed the robustness of our staining by confirming Edu positive cells in intestinal villi, a region with high levels of cell proliferation (**Figure 6A)**. In female brains, the densities of Edu positive cells and DCX positive cells did not differ between *Ins2*$^{-/-}$ and *Ins2*$^{+/+}$ mice, in either the dorsal or ventral dentate gyrus (**Figure 6B-D**). In male brains, *Ins2*$^{-/-}$ mice had a larger density of EdU positive cells in the dorsal ($F(1,10) = 5.57$, $p<0.05$)(**Figure 6C**), but not ventral hippocampus (**Figure 6D**). One could speculate that this may represent compensation that may prevent male *Ins2*$^{-/-}$ mice from exhibiting defects in learning and memory. The density of DCX cells did not differ between *Ins2*$^{-/-}$ and Ins2$^{+/+}$ male mice in either the dorsal or ventral hippocampus (**Figure 6E,F**). Together, these data suggest that adult neurogenesis, measured at this late stage of life, is not a major factor in differences in learning and memory in female *Ins2*$^{-/-}$ mice.

Discussion

The objectives of this study were to further elucidate the expression of insulin in the hippocampus and to determine the role of brain-produced insulin on hippocampus-dependent learning and memory. Using *Ins2* knockout with devoid of hippocampal pro-insulin, but with limited effects on peripheral metabolism, we defined a female-specific role for brain-insulin production in learning and memory.

Given that *Ins2* is expressed in both the brain and pancreas, it was important to assess the effect of *Ins2* knockout on peripheral metabolism, which could theoretically affect brain function indirectly. In-depth metabolic characterization of *Ins2*$^{-/-}$ and *Ins2*$^{+/+}$ mice showed that they were similar in most measures of metabolism, including body weight, glucose tolerance and insulin tolerance tests. Together these results suggest that the changes in *Ins2* expression and behavioral impairments observed in *Ins2*$^{-/-}$ mice are likely not due to peripheral metabolic dysfunction. The relatively few metabolic changes in

Ins2$^{-/-}$ mice indicates that the *Ins1* allele can produce a near-complete compensation for the loss of *Ins2* in the context of the diet and housing conditions used in our study, and that this compensation can be maintained through aging. The mechanism for this compensation is largely unexplored but is likely supported by elevated *Ins1* expression within the pancreas and pancreatic β-cell hyperplasia (39). This is likely due to inter-allelic redundancy and compensation within the pancreas, where both alleles contribute to insulin production, and may be especially important under periods of metabolic stress. Indeed, we found that metabolic changes in *Ins2*$^{-/-}$ mice were present only at 16-18 months, when the accumulated stressors associated with aging were expected to be the largest. However, given that *Ins2* is also expressed in the brain, we cannot rule out that loss of brain-produced insulin also contributed to the few metabolic differences observed in *Ins2*$^{-/-}$ mice.

To the best of our knowledge, this is the first time cognitive behaviour has been examined in the context of genetic insulin reduction. Our study was also unique in that we deleted only *Ins2*, resulting in brain-selective insulin knockout. To contextualize our knockout model, we extended on our previous work that provided conclusive evidence, using knockout controls, that insulin is produce locally in the brain, and more prominently in the hippocampus relative to other brain regions (25). Other work has examined *Ins2* expression and insulin synthesis across different brain regions in a plethora of animal models (23, 24, 26, 46-48). Studies that include hippocampal regions consistently report elevated levels of insulin expression relative to other brain regions suggesting a role for local *Ins2* production in hippocampal function (12, 25). This is further supported by *in vitro* studies reporting *Ins2* expression and insulin synthesis within cultured primary hippocampal neurons (49, 50). Importantly, we confirmed that Ins2 protein is found in the hippocampus of wildtype but not *Ins2* knockout mice. Moreover, we show that female mice show higher *Ins2* expression than males in both the hippocampus and cerebellum. There are currently very few studies that examine sex differences in *Ins2* expression within the brain, and to the best of our knowledge, this is the first study to show that *Ins2* expression within the hippocampus is sexually dimorphic. It had been proposed that insulin within the brain can be modulated by environmental factors including diet (51), and here we show that environmental effects on *Ins2* brain expression are also sexual dimorphic.

Women are at higher risk at younger ages to develop Alzheimer's disease (52). Consistent with this, we found evidence for a female-specific role of brain-derived insulin in hippocampal-dependent learning and memory, particularly in spatial-visual tasks. It has been suggested that male rodents have better spatial abilities like spatial working memory and orientation, whereas females are better in location memory (53). In our experiments, there were not significant differences in learning or memory measures between male and female wildtype mice. When compared to other studies, it should be noted that our experiments were conducted on older mice, which is more relevant to Alzeimer's disease.

The ability to perform tasks of learning can be influenced by non-cognitive factors, thus potentially confounding measures of learning and memory (54). For example, performance on the Morris water maze can be influenced by differences in stress reactivity, motivation to locate the escape platform, impaired visual ability and impaired swimming ability due to motor dysfunction (55). The similar anxiety-like behavioural profiles in female *Ins2*$^{-/-}$ and *Ins2*$^{+/+}$ mice suggests that our reported differences in visuo-spatial learning and memory are not likely due to pre-existing differences in stress reactivity within the water maze. This is further supported by the lack of differences in swim-speed observed in the water maze indicating unimpaired swimming ability and similar motivation to locate the escape platform. Therefore, these results provide additional confidence that differences in learning and memory on the water maze in female *Ins2*$^{-/-}$ mice were not due to potential non-cognitive factors influencing performance.

The functional role of the hippocampus has been proposed to differ along the dorso-ventral axis, with the dorsal hippocampus involved moreso in cognitive function, and the ventral hippocampus involved in stress and emotionality. Given that female *Ins2*$^{-/-}$ mice showed impaired learning and memory, we also examined if differences extended to anxiety-like behaviour. We did not observe any differences in anxiety-like behaviour in either male or female *Ins2*$^{-/-}$ mice. We should note, however, that over-expressing *Ins2* within the choroid plexus is sufficient to reduce anxiety-like behaviour, but only when mice are given a high-fat diet (27). This may indicate a role for *Ins2* in regulating other brain behaviours, including anxiety, specifically during metabolic challenges.

The *Ins2* knockout mouse model in this study is most appropriate to directly test the effects of endogenous insulin of the brain to date. Silencing the *Ins2* gene, while keeping *Ins1* intact, allows to specifically examine the causal effects of insulin synthesis in the brain independent of peripheral insulin. However, our model does not come without its own limitations. The *Ins2* gene is also, in addition to the pancreas and brain, expressed in the thymus. The thymus is most known for its role in immunity and insulin deletion in the thymus can induce autoimmune diabetes (56). Thus, with a global *Ins2* knockout, it cannot be entirely excluded that the results of this study are exclusively due to brain-insulin loss but may indirectly relate to immune dysfunction. Generating tissue-specific *Ins2* knockout could be used to circumvent this limitation, but our efforts to do so have been unsuccessful. Another limitation of our study was that the loss of *Ins2* was lifelong. Future studies could employ a floxed *Ins2* allele and brain-specific Cre viral vectors or drug-inducible transgenes in mice to remove *Ins2* in the adult brain, in a region-specific manner. Other methods of acutely testing for local brain insulin ablated insulin-expressing neurons with the beta-cell toxin streptozotocin (57-59). However, toxic drugs may also affect other areas of the brain, and it would be difficult to say whether effects on behavior are due to brain-derived insulin loss or generalized toxicity. Our work also does not identify the cellular target(s) of local insulin production, not their molecular mechanisms. Insulin receptors have been shown to mediate important roles of insulin in many neuronal cell populations in the brain, including the hippocampus (60-62). Insulin also acts directly though insulin receptors to modulate the activity of non-neuronal brain cells including astrocytes (63-65). Indeed, inducible loss of insulin action via insulin receptor and IGF1 receptor deletion in astrocytes significantly worsened multiple Alzheimer's pathologies in a mouse model (10). In a recent study, cerebrovascular insulin receptors were also shown to be deficient in Alzheimer's disease (66). Clearly, more research will be required to fully elucidate local insulin-insulin receptor trophic circuits across multiple cell types in the brain.

In conclusion, we confirmed that *Ins2* is produced in the hippocampus and discovered a significant sex difference in mRNA levels. This study used a genetic model of *Ins2* deletion to assess the influence of brain insulin production, in the absence of major metabolic disturbances. We also showed for the first time that insulin produced in the brain plays an important role in spatial navigation in female mice.

References

1. Hölscher, C. (2011) Diabetes as a risk factor for Alzheimer's disease: insulin signalling impairment in the brain as an alternative model of Alzheimer's disease. Portland Press Ltd.
2. Ryan, C. M., and Geckle, M. (2000) Why is learning and memory dysfunction in Type 2 diabetes limited to older adults? *Diabetes/metabolism research and reviews* **16**, 308-315
3. De Felice, F. G., Lourenco, M. V., and Ferreira, S. T. (2014) How does brain insulin resistance develop in Alzheimer's disease? *Alzheimer's & Dementia* **10**, S26-S32
4. Talbot, K., Wang, H.-Y., Kazi, H., Han, L.-Y., Bakshi, K. P., Stucky, A., Fuino, R. L., Kawaguchi, K. R., Samoyedny, A. J., Wilson, R. S., Arvanitakis, Z., Schneider, J. A., Wolf, B. A., Bennett, D. A., Trojanowski, J. Q., and Arnold, S. E. (2012) Demonstrated brain insulin resistance in Alzheimer's disease patients is associated with IGF-1 resistance, IRS-1 dysregulation, and cognitive decline. *Journal of Clinical Investigation* **122**, 1316-1338
5. Forner, S., Baglietto-Vargas, D., Martini, A. C., Trujillo-Estrada, L., and LaFerla, F. M. (2017) Synaptic Impairment in Alzheimer's Disease: A Dysregulated Symphony. *Trends Neurosci* **40**, 347-357
6. Kellar, D., and Craft, S. (2020) Brain insulin resistance in Alzheimer's disease and related disorders: mechanisms and therapeutic approaches. *Lancet Neurol* **19**, 758-766
7. Laws, S. M., Gaskin, S., Woodfield, A., Srikanth, V., Bruce, D., Fraser, P. E., Porter, T., Newsholme, P., Wijesekara, N., and Burnham, S. (2017) Insulin resistance is associated with reductions in specific cognitive domains and increases in CSF tau in cognitively normal adults. *Scientific reports* **7**, 1-11
8. Ma, L., Wang, J., and Li, Y. (2015) Insulin resistance and cognitive dysfunction. *Clinica chimica acta* **444**, 18-23

9. Talbot, K., Wang, H.-Y., Kazi, H., Han, L.-Y., Bakshi, K. P., Stucky, A., Fuino, R. L., Kawaguchi, K. R., Samoyedny, A. J., and Wilson, R. S. (2012) Demonstrated brain insulin resistance in Alzheimer's disease patients is associated with IGF-1 resistance, IRS-1 dysregulation, and cognitive decline. *The Journal of clinical investigation* **122**, 1316-1338
10. Chen, W., Huang, Q., Lazdon, E. K., Gomes, A., Wong, M., Stephens, E., Royal, T. G., Frenkel, D., Cai, W., and Kahn, C. R. (2023) Loss of insulin signaling in astrocytes exacerbates Alzheimer-like phenotypes in a 5xFAD mouse model. *Proceedings of the National Academy of Sciences* **120**, e2220684120
11. Cai, W., Xue, C., Sakaguchi, M., Konishi, M., Shirazian, A., Ferris, H. A., Li, M. E., Yu, R., Kleinridders, A., and Pothos, E. N. (2018) Insulin regulates astrocyte gliotransmission and modulates behavior. *The Journal of clinical investigation* **128**, 2914-2926
12. Kuwabara, T., Kagalwala, M. N., Onuma, Y., Ito, Y., Warashina, M., Terashima, K., Sanosaka, T., Nakashima, K., Gage, F. H., and Asashima, M. (2011) Insulin biosynthesis in neuronal progenitors derived from adult hippocampus and the olfactory bulb. *EMBO Mol Med* **3**, 742-754
13. Devaskar, S. U., Giddings, S. J., Rajakumar, P. A., Carnaghi, L. R., Menon, R. K., and Zahm, D. S. (1994) Insulin gene expression and insulin synthesis in mammalian neuronal cells. *J Biol Chem* **269**, 8445-8454
14. Freiherr, J., Hallschmid, M., Frey, W. H., Brünner, Y. F., Chapman, C. D., Hölscher, C., Craft, S., De Felice, F. G., and Benedict, C. (2013) Intranasal insulin as a treatment for Alzheimer's disease: a review of basic research and clinical evidence. *CNS drugs* **27**, 505-514
15. Zhang, H., Hao, Y., Manor, B., Novak, P., Milberg, W., Zhang, J., Fang, J., and Novak, V. (2015) Intranasal insulin enhanced resting-state functional connectivity of hippocampal regions in type 2 diabetes. *Diabetes* **64**, 1025-1034
16. Li, X., Yang, Y., Bai, X., Wang, X., Tan, H., Chen, Y., Zhu, Y., Liu, Q., Wu, M. N., and Li, Y. (2024) A brain-derived insulin signal encodes protein satiety for nutrient-specific feeding inhibition. *Cell Rep* **43**, 114282
17. Born, J., Lange, T., Kern, W., McGregor, G. P., Bickel, U., and Fehm, H. L. (2002) Sniffing neuropeptides: a transnasal approach to the human brain. *Nature Neuroscience* **5**, 514-516
18. Ko, Y., and Chye, S. M. (2020) Lifestyle intervention to prevent Alzheimer's disease. *Reviews in the Neurosciences* **31**, 817-824
19. Braak, H., and Braak, E. (1995) Staging of Alzheimer's disease-related neurofibrillary changes. *Neurobiology of aging* **16**, 271-278
20. Gray, S. M., Aylor, K. W., and Barrett, E. J. (2017) Unravelling the regulation of insulin transport across the brain endothelial cell. *Diabetologia* **60**, 1512-1521
21. Dakic, T., Jevdjovic, T., Lakic, I., Ruzicic, A., Jasnic, N., Djurasevic, S., Djordjevic, J., and Vujovic, P. (2023) The Expression of Insulin in the Central Nervous System: What Have We Learned So Far? *International Journal of Molecular Sciences* **24**, 6586
22. Molnar, G., Farago, N., Kocsis, A. K., Rozsa, M., Lovas, S., Boldog, E., Baldi, R., Csajbok, E., Gardi, J., Puskas, L. G., and Tamas, G. (2014) GABAergic neurogliaform cells represent local sources of insulin in the cerebral cortex. *J Neurosci* **34**, 1133-1137
23. Nemoto, T., Toyoshima-Aoyama, F., Yanagita, T., Maruta, T., Fujita, H., Koshida, T., Yonaha, T., Wada, A., Sawaguchi, A., and Murakami, M. (2014) New insights concerning insulin synthesis and its secretion in rat hippocampus and cerebral cortex: amyloid-beta1-42-induced reduction of proinsulin level via glycogen synthase kinase-3beta. *Cell Signal* **26**, 253-259
24. Mazucanti, C. H., Liu, Q. R., Lang, D., Huang, N., O'Connell, J. F., Camandola, S., and Egan, J. M. (2019) Release of insulin produced by the choroid plexis is regulated by serotonergic signaling. *JCI Insight* **4**
25. Mehran, A. E., Templeman, N. M., Brigidi, G. S., Lim, G. E., Chu, K. Y., Hu, X., Botezelli, J. D., Asadi, A., Hoffman, B. G., Kieffer, T. J., Bamji, S. X., Clee, S. M., and Johnson, J. D. (2012) Hyperinsulinemia drives diet-induced obesity independently of brain insulin production. *Cell Metab* **16**, 723-737

26. Lee, J., Kim, K., Cho, J. H., Bae, J. Y., O'Leary, T. P., Johnson, J. D., Bae, Y. C., and Kim, E. K. (2020) Insulin synthesized in the paraventricular nucleus of the hypothalamus regulates pituitary growth hormone production. *JCI Insight* **5**
27. Mazucanti, C. H., Kennedy, V., Jr., Premathilake, H. U., Doyle, M. E., Tian, J., Liu, Q. R., O'Connell, J., Camandola, S., and Egan, J. M. (2023) AAV5-mediated manipulation of insulin expression in choroid plexus has long-term metabolic and behavioral consequences. *Cell Rep* **42**, 112903
28. Duvillie, B., Cordonnier, N., Deltour, L., Dandoy-Dron, F., Itier, J. M., Monthioux, E., Jami, J., Joshi, R. L., and Bucchini, D. (1997) Phenotypic alterations in insulin-deficient mutant mice. *Proc Natl Acad Sci U S A* **94**, 5137-5140
29. Berdugo-Vega, G., Dhingra, S., and Calegari, F. (2023) Sharpening the blades of the dentate gyrus: how adult-born neurons differentially modulate diverse aspects of hippocampal learning and memory. *Embo J* **42**, e113524
30. Hitoshi, S., Mandyam, C. D., and Shetty, A. K. (2023) Editorial: Advances in adult neurogenesis. *Front Neurosci* **17**, 1307844
31. Brooker, G. J., Kalloniatis, M., Russo, V. C., Murphy, M., Werther, G. A., and Bartlett, P. F. (2000) Endogenous IGF-1 regulates the neuronal differentiation of adult stem cells. *Journal of neuroscience research* **59**, 332-341
32. Åberg, M. A., Åberg, N. D., Palmer, T. D., Alborn, A.-M., Carlsson-Skwirut, C., Bang, P., Rosengren, L. E., Olsson, T., Gage, F. H., and Eriksson, P. S. (2003) IGF-I has a direct proliferative effect in adult hippocampal progenitor cells. *Molecular and Cellular Neuroscience* **24**, 23-40
33. Duvillié, B., Cordonnier, N., Deltour, L., Dandoy-Dron, F., Itier, J.-M., Monthioux, E., Jami, J., Joshi, R. L., and Bucchini, D. (1997) Phenotypic alterations in insulin-deficient mutant mice. *Proceedings of the National Academy of Sciences* **94**, 5137-5140
34. Chu, C. M. J., Modi, H., Ellis, C., Krentz, N. A. J., Skovso, S., Zhao, Y. B., Cen, H., Noursadeghi, N., Panzhinskiy, E., Hu, X., Dionne, D. A., Xia, Y. H., Xuan, S., Huising, M. O., Kieffer, T. J., Lynn, F. C., and Johnson, J. D. (2022) Dynamic Ins2 Gene Activity Defines beta-Cell Maturity States. *Diabetes* **71**, 2612-2631
35. Kim, S., Kim, N., Park, S., Jeon, Y., Lee, J., Yoo, S. J., Lee, J. W., Moon, C., Yu, S. W., and Kim, E. K. (2020) Tanycytic TSPO inhibition induces lipophagy to regulate lipid metabolism and improve energy balance. *Autophagy* **16**, 1200-1220
36. Ritchie, M. E., Phipson, B., Wu, D., Hu, Y., Law, C. W., Shi, W., and Smyth, G. K. (2015) limma powers differential expression analyses for RNA-sequencing and microarray studies. *Nucleic Acids Research* **43**, e47-e47
37. Love, M. I., Huber, W., and Anders, S. (2014) Moderated estimation of fold change and dispersion for RNA-seq data with DESeq2. *Genome Biol* **15**, 550
38. Yu, G., Wang, L. G., Han, Y., and He, Q. Y. (2012) clusterProfiler: an R package for comparing biological themes among gene clusters. *OMICS* **16**, 284-287
39. Leroux, L., Desbois, P., Lamotte, L., Duvillie, B., Cordonnier, N., Jackerott, M., Jami, J., Bucchini, D., and Joshi, R. L. (2001) Compensatory responses in mice carrying a null mutation for Ins1 or Ins2. *Diabetes* **50 Suppl 1**, S150-153
40. Vorhees, C. V., and Williams, M. T. (2014) Assessing spatial learning and memory in rodents. *Ilar j* **55**, 310-332
41. D'Hooge, R., and De Deyn, P. P. (2001) Applications of the Morris water maze in the study of learning and memory. *Brain Res Brain Res Rev* **36**, 60-90
42. Bannerman, D. M., Grubb, M., Deacon, R. M., Yee, B. K., Feldon, J., and Rawlins, J. N. (2003) Ventral hippocampal lesions affect anxiety but not spatial learning. *Behav Brain Res* **139**, 197-213
43. Fanselow, M. S., and Dong, H. W. (2010) Are the dorsal and ventral hippocampus functionally distinct structures? *Neuron* **65**, 7-19
44. Liu, Z., Wan, X., Chen, J., Ma, Y., Fu, Y., Chen, Y., Wen, M., Yang, Y., Qian, Y., Zhang, Y., Zhu, D., Li, J., Jing, N., and Yang, X. (2025) Genomic locus of lncRNA-Gm26793 forms an

inter-chromosomal interaction with Cubn to ensure proper stem cell differentiation in vitro and in vivo. *Cell Discov* **11**, 53
45. Milstein, J. L., and Ferris, H. A. (2021) The brain as an insulin-sensitive metabolic organ. *Mol Metab* **52**, 101234
46. Young III, W. S. (1986) Periventricular hypothalamic cells in the rat brain contain insulin mRNA. *Neuropeptides* **8**, 93-97
47. Havrankova, J., Schmechel, D., Roth, J., and Brownstein, M. (1978) Identification of insulin in rat brain. *Proceedings of the National Academy of Sciences* **75**, 5737-5741
48. Csajbok, E. A., and Tamas, G. (2016) Cerebral cortex: a target and source of insulin? *Diabetologia* **59**, 1609-1615
49. Kuwabara, T., Kagalwala, M. N., Onuma, Y., Ito, Y., Warashina, M., Terashima, K., Sanosaka, T., Nakashima, K., Gage, F. H., and Asashima, M. (2011) Insulin biosynthesis in neuronal progenitors derived from adult hippocampus and the olfactory bulb. *EMBO Molecular Medicine* **3**, 742-754
50. Nemoto, T., Toyoshima-Aoyama, F., Yanagita, T., Maruta, T., Fujita, H., Koshida, T., Yonaha, T., Wada, A., Sawaguchi, A., and Murakami, M. (2014) New insights concerning insulin synthesis and its secretion in rat hippocampus and cerebral cortex: Amyloid-β1–42-induced reduction of proinsulin level via glycogen synthase kinase-3β. *Cellular Signalling* **26**, 253-259
51. de la Monte, S. M., Tong, M., Bowling, N., and Moskal, P. (2011) si-RNA inhibition of brain insulin or insulin-like growth factor receptors causes developmental cerebellar abnormalities: relevance to fetal alcohol spectrum disorder. *Mol Brain* **4**, 13
52. Neu, S. C., Pa, J., Kukull, W., Beekly, D., Kuzma, A., Gangadharan, P., Wang, L.-S., Romero, K., Arneric, S. P., and Redolfi, A. (2017) Apolipoprotein E genotype and sex risk factors for Alzheimer disease: a meta-analysis. *JAMA neurology* **74**, 1178-1189
53. Fleischer, A. W., and Frick, K. M. (2023) New perspectives on sex differences in learning and memory. *Trends in Endocrinology & Metabolism* **34**, 526-538
54. Cahill, L., McGaugh, J. L., and Weinberger, N. M. (2001) The neurobiology of learning and memory: some reminders to remember. *Trends Neurosci* **24**, 578-581
55. O'Leary, T. P., and Brown, R. E. (2022) Visuo-spatial learning and memory impairments in the 5xFAD mouse model of Alzheimer's disease: Effects of age, sex, albinism, and motor impairments. *Genes Brain Behav* **21**, e12794
56. Fan, Y., Rudert, W. A., Grupillo, M., He, J., Sisino, G., and Trucco, M. (2009) Thymus-specific deletion of insulin induces autoimmune diabetes. *The EMBO Journal* **28**, 2812-2824
57. Grünblatt, E., Salkovic-Petrisic, M., Osmanovic, J., Riederer, P., and Hoyer, S. (2007) Brain insulin system dysfunction in streptozotocin intracerebroventricularly treated rats generates hyperphosphorylated tau protein. *Journal of neurochemistry* **101**, 757-770
58. Plaschke, K., Kopitz, J., Siegelin, M., Schliebs, R., Salkovic-Petrisic, M., Riederer, P., and Hoyer, S. (2010) Insulin-resistant brain state after intracerebroventricular streptozotocin injection exacerbates Alzheimer-like changes in Tg2576 AβPP-overexpressing mice. *Journal of Alzheimer's disease* **19**, 691-704
59. Lester-Coll, N., Rivera, E. J., Soscia, S. J., Doiron, K., Wands, J. R., and de la Monte, S. M. (2006) Intracerebral streptozotocin model of type 3 diabetes: relevance to sporadic Alzheimer's disease. *Journal of Alzheimer's Disease* **9**, 13-33
60. Chen, W., Cai, W., Hoover, B., and Kahn, C. R. (2022) Insulin action in the brain: cell types, circuits, and diseases. *Trends Neurosci* **45**, 384-400
61. Dixon-Salazar, T. J., Fourgeaud, L., Tyler, C. M., Poole, J. R., Park, J. J., and Boulanger, L. M. (2014) MHC class I limits hippocampal synapse density by inhibiting neuronal insulin receptor signaling. *J Neurosci* **34**, 11844-11856
62. Soto, M., Cai, W., Konishi, M., and Kahn, C. R. (2019) Insulin signaling in the hippocampus and amygdala regulates metabolism and neurobehavior. *Proceedings of the National Academy of Sciences* **116**, 6379-6384

63. Cai, W., Xue, C., Sakaguchi, M., Konishi, M., Shirazian, A., Ferris, H. A., Li, M. E., Yu, R., Kleinridders, A., Pothos, E. N., and Kahn, C. R. (2018) Insulin regulates astrocyte gliotransmission and modulates behavior. *J Clin Invest* **128**, 2914-2926
64. Taib, B., Deme, P., Gupta, S., Yoo, S. W., Khuder, S. S., Hoke, A., Li, Z., Ahima, R. S., and Haughey, N. J. (2025) Insulin acts on astrocytes to shift their substrate preference to fatty acids. *iScience* **28**, 111642
65. Fernandez, A. M., Martinez-Rachadell, L., Navarrete, M., Pose-Utrilla, J., Davila, J. C., Pignatelli, J., Diaz-Pacheco, S., Guerra-Cantera, S., Viedma-Moreno, E., Palenzuela, R., Ruiz de Martin Esteban, S., Mostany, R., Garcia-Caceres, C., Tschöp, M., Iglesias, T., de Ceballos, M. L., Gutierrez, A., and Torres Aleman, I. (2022) Insulin regulates neurovascular coupling through astrocytes. *Proc Natl Acad Sci U S A* **119**, e2204527119
66. Leclerc, M., Bourassa, P., Tremblay, C., Caron, V., Sugère, C., Emond, V., Bennett, D. A., and Calon, F. (2022) Cerebrovascular insulin receptors are defective in Alzheimer's disease. *Brain* **146**, 75-90

Figure Legends

Figure 1. Specific *Ins2* protein immunoreactivity in the mouse brain. (A) Immunoreactivity for C-peptide, a product of insulin biosynthesis, is detected in the hilus, stratum lucidum (SL), and CA3 regions of hippocampus. C-peptide immunoreactive cells were observed in the granule cell layer of the dentate gyrus, as indicated by arrows. **(B)** Immunoblot analysis of proinsulin expression in the pancreas and hippocampus from WT and *Ins2* KO mice. **(C)** Proinsulin-positive cells were detected and co-localized with β-gal in the CA3 regions. β-galactosidase (β-gal) staining was detected in *Ins2* knockout and heterozygous mice but not wildtype (WT). Pro-insulin was detected in WT and β-gal heterozygous mice but not knockouts. **(D)** GFP fluorescence in hippocampal neuron cultures of from *Ins2*$^{GFP/GFP}$ knock-in, replacement mice.

Figure 2. *Ins2* expression in the brain is sexually dimorphic and is modulated by diet in female mice. (A) *Ins2* gene expression in male and female mice across multiple brain regions, including the hippocampus, cerebellum, cerebral cortex, olfactory bulb, hypothalamus and midbrain (all remaining tissue). *Ins2* expression was normalized to beta-actin expression within each region. **(B,C)** *Ins2* expression in the hippocampus and cerebral cortex of male and female mice fed high-fat or control chow diets. **=p<.005, ***=p<.0001.

Figure 3. Metabolic profile of young and old *Ins2* knockout mice. (A,B) Body weight of male and female *Ins2*$^{-/-}$ mice did not differ from *Ins2*$^{+/+}$ mice at any of the ages measured. **(C,D)** Fasted (4 hours) blood glucose levels were largely similar between *Ins2*$^{-/-}$ and *Ins2*$^{+/+}$ mice and differed only in males at the oldest age (16-18 months) measured. **(E-L)** *Ins2*$^{-/-}$ and *Ins2*$^{+/+}$ mice did not differ in either glucose tolerance or insulin tolerance tests. **(M-P)** *Ins2*$^{-/-}$ and *Ins2*$^{+/+}$ mice were also similar in glucose stimulated insulin secretion, although there was a trend for higher insulin in female *Ins2*$^{+/+}$ than *Ins2*$^{-/-}$ mice in old age (16-18 months).

Figure 4. Visuo-spatial learning and memory is impaired in female *Ins2*$^{-/-}$, but not in male *Ins2*$^{-/-}$ mice. (A) Latency to locate the escape platform in female *Ins2*$^{-/-}$ mice and *Ins2*$^{+/+}$ mice during acquisition (A1-6), re-training (RT) and reversal training (R1-6). Performance for the first 3 days and last 3 days of acquisition and reversal training were analyzed separately (indicated by horizontal dashed line). **(B)** Cumulative search error for female *Ins2*$^{-/-}$ and *Ins2*$^{+/+}$ mice on the same study days. **(C)** The number of platform annulus crossings completed by female *Ins2*$^{-/-}$ and *Ins2*$^{+/+}$ mice during the acquisition probe trial. **(D)** Distance travelled by female *Ins2*$^{-/-}$ and *Ins2*$^{+/+}$ mice to reach the escape platform on each study day. **(E)** Swim-speed for female *Ins2*$^{-/-}$ and *Ins2*$^{+/+}$ mice over acquisition and reversal training. **(F)** Platform annulus crossings during the reversal probe trial. **(G-L)** Show the same measurements as above, but for male mice. *=p<.05

Figure 5. Bulk mRNA sequencing and cluster analysis of isolated *Ins2*$^{-/-}$ and *Ins2*$^{+/+}$ hippocampi from female mice. (A) Cluster dendrogram and **(B)** PCA showing the 3 outlier samples. **(C)** Bulk mRNA sequencing shows no *Ins2* mRNA for *Ins2* knockouts **(D)** Differentially expressed genes ranked from most significantly downregulated to upregulated (top to bottom). **(E)** Gene set enrichment analysis using Gene Ontology - Biological Process (FDR< 0.0001).

Figure 6. Effects of *Ins2* loss on adult hippocampal neurogenesis in aged male and female mice. (A) Specific labeling of EdU in the intestine, our positive control for proliferating cells in aged animals. **(B)** Co-labeling of EdU and DCX markers in the dentate gyrus of the hippocampus. **(C,D)** Quantification of the density of EdU^{+} cells in the dorsal and ventral dentate gyrus in *Ins2*$^{-/-}$ and *Ins2*$^{+/+}$ mice. **(E,F)** Quantification of the density of DCX^{+} cells in the dorsal and ventral dentate gyrus.*=p<.05

Supplemental Figure 1. *Ins2*$^{-/-}$ and *Ins2*$^{+/+}$ mice do not differ in anxiety-like behaviour or locomotor activity. **(A-C)** Anxiety-like behaviour in male and female, *Ins2*$^{-/-}$ and *Ins2*$^{+/+}$ mice (time in anxiogenic regions) on each of the open-field, light-dark box and elevated-plus maze. **(D-F)** Locomotor activity in male and female, *Ins2*$^{-/-}$ and *Ins2*$^{+/+}$ mice (time in anxiogenic regions) on each of the open-field, light-dark box and elevated-plus maze. **(G-I)** Measures of species-typical behaviours (rears, grooming, freezing) in the open-field. **(J-L)** Measures of species-typical behaviours (rears, grooming, freezing) in the light-dark box. **(M-P)** Measures of species-typical behaviours (rears, grooming, freezing, open-arm, head-dips) in the elevated plus maze.

Figure 1

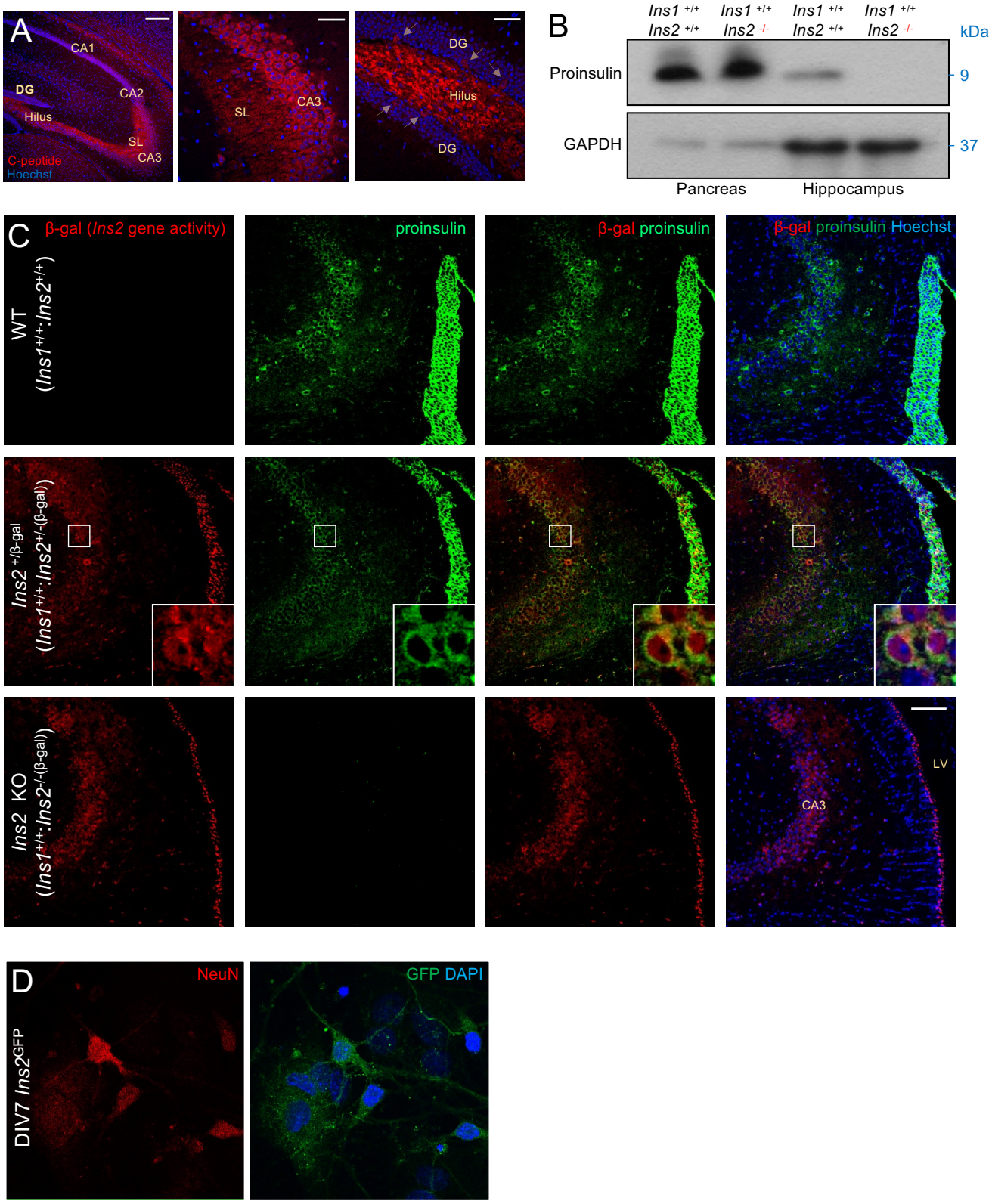
A
CA1
DG
CA2
Hilus
SL
CA3
C-peptide
Hoechst
SL
CA3
DG
Hilus
DG
B
Ins1 +/+ Ins2 +/+
Ins1 +/+ Ins2 -/-
Ins1 +/+ Ins2 +/+
Ins1 +/+ Ins2 -/-
kDa
Proinsulin
9
GAPDH
37
Pancreas
Hippocampus
C
β-gal (Ins2 gene activity)
proinsulin
β-gal proinsulin
β-gal proinsulin Hoechst
WT
(Ins1+/+:Ins2+/+)
Ins2 +/β-gal
(Ins1+/+:Ins2+/-(β-gal))
Ins2 KO
(Ins1+/+:Ins2-/-(β-gal))
LV
CA3
D
NeuN
GFP DAPI
DIV7 Ins2GFP

Figure 2

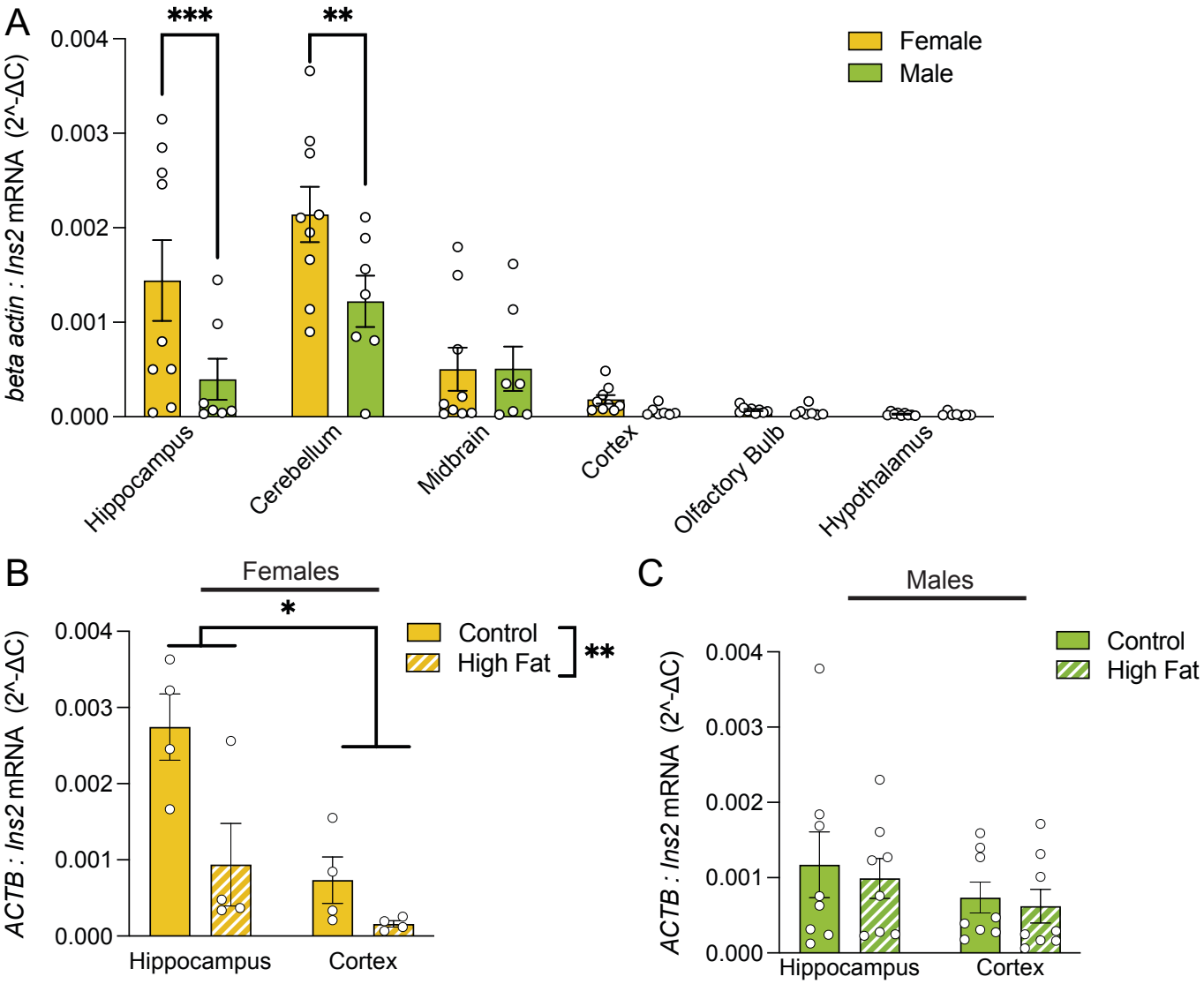
A
***
**
Female
Male
beta actin : Ins2 mRNA (2^-ΔC)
0.004
0.003
0.002
0.001
0.000
Hippocampus
Cerebellum
Midbrain
Cortex
Olfactory Bulb
Hypothalamus
B
Females
*
Control
High Fat
**
ACTB : Ins2 mRNA (2^-ΔC)
0.004
0.003
0.002
0.001
0.000
Hippocampus
Cortex
C
Males
Control
High Fat
ACTB : Ins2 mRNA (2^-ΔC)
0.004
0.003
0.002
0.001
0.000
Hippocampus
Cortex

Figure 3

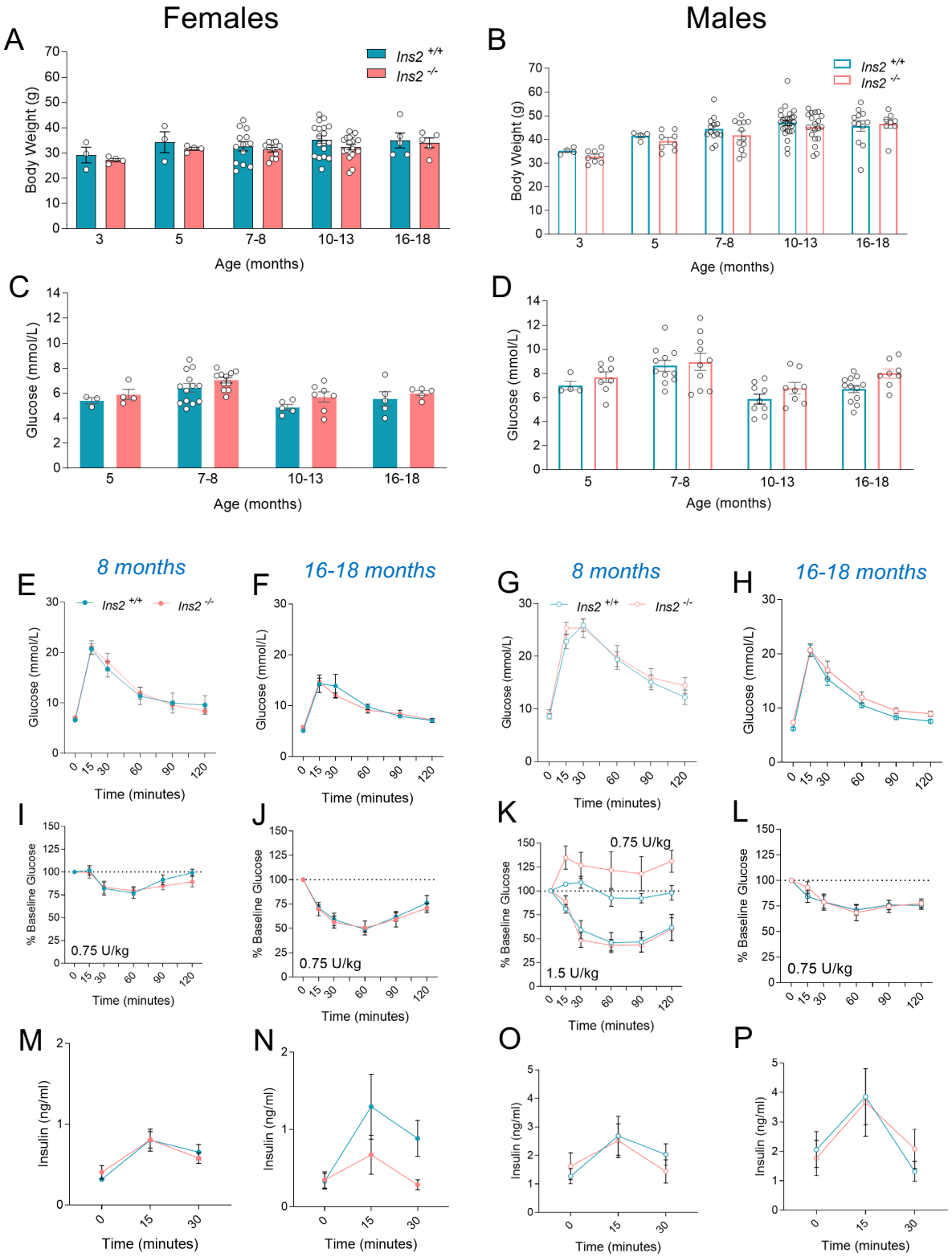
Females
Males
A
B
C
D
Ins2 +/+
Ins2 -/-
Body Weight (g)
Glucose (mmol/L)
Age (months)
3
5
7-8
10-13
16-18
E
F
G
H
8 months
16-18 months
Time (minutes)
I
J
K
L
% Baseline Glucose
0.75 U/kg
1.5 U/kg
M
N
O
P
Insulin (ng/ml)

Figure 4

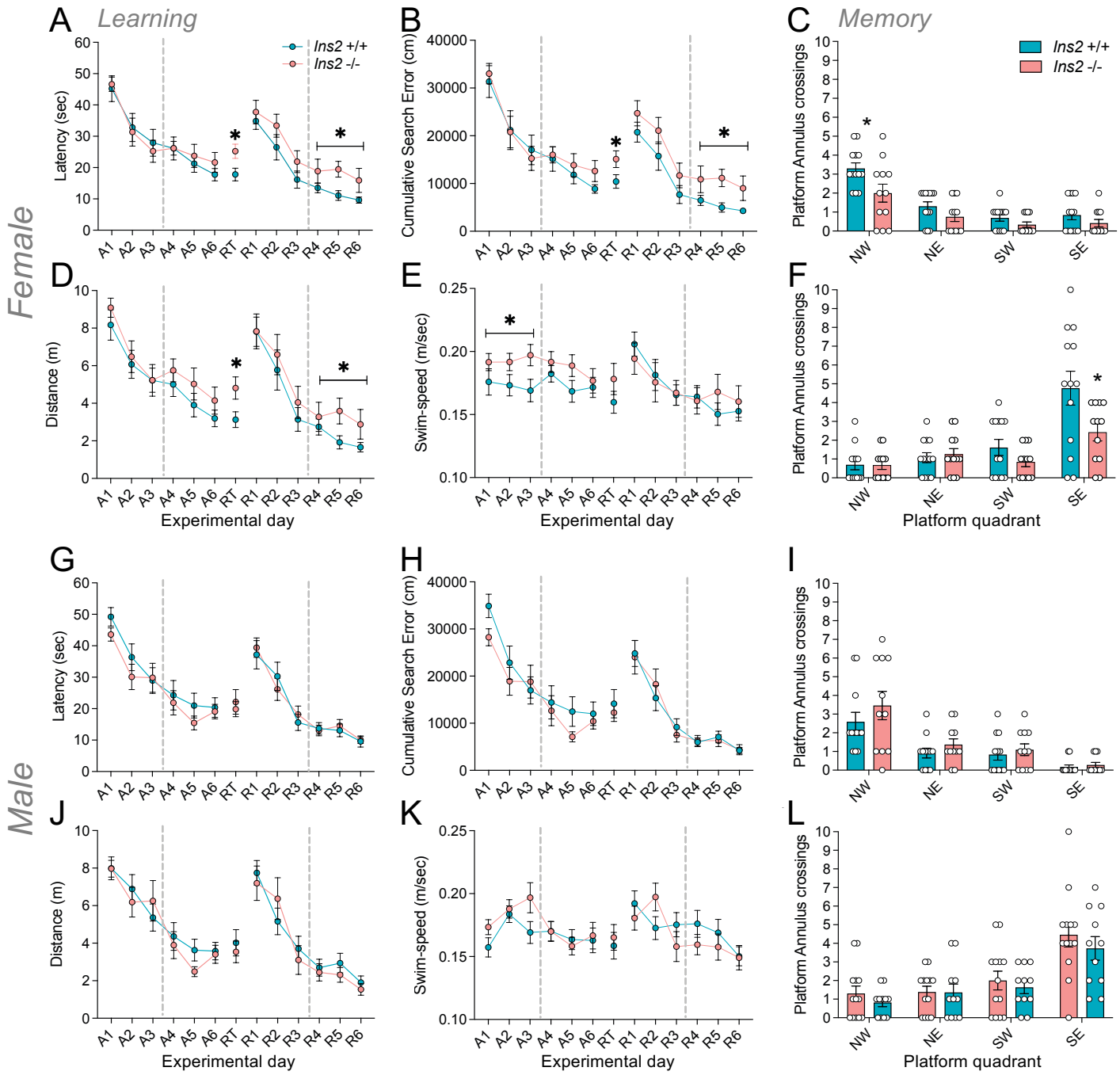
A
Learning
Ins2 +/+
Ins2 -/-
Latency (sec)
B
Cumulative Search Error (cm)
C
Memory
Platform Annulus crossings
Female
D
Distance (m)
Experimental day
E
Swim-speed (m/sec)
F
Platform quadrant
NW
NE
SW
SE
Male
G
H
I
J
K
L
A1 A2 A3 A4 A5 A6 RT R1 R2 R3 R4 R5 R6

Figure 5

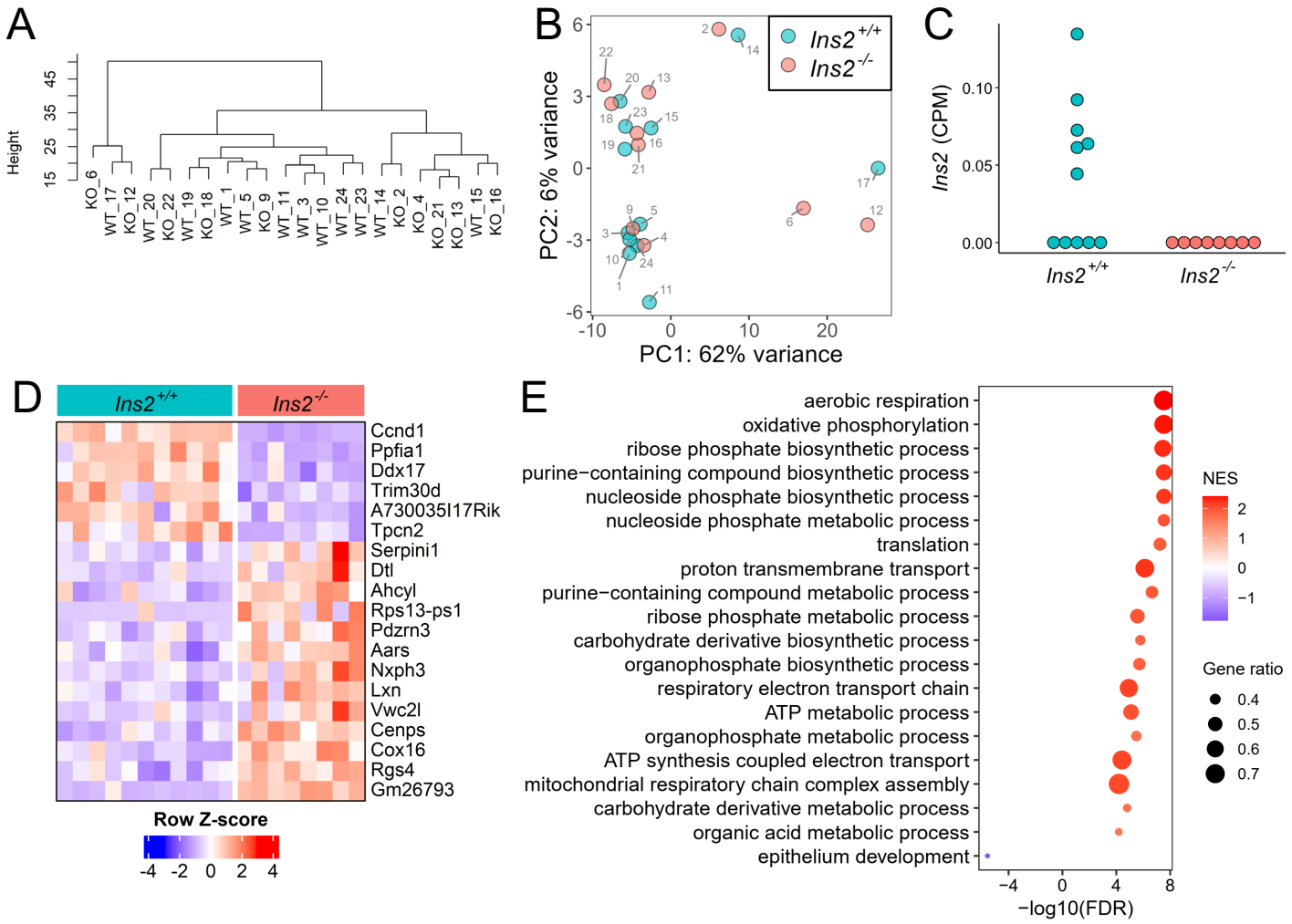
A
Height
15
25
35
45
KO_6
WT_17
KO_12
WT_20
KO_22
WT_19
KO_18
WT_1
WT_5
KO_9
WT_11
WT_3
WT_10
WT_24
WT_23
WT_14
KO_2
KO_4
KO_21
KO_13
WT_15
KO_16
B
Ins2+/+
Ins2-/-
PC2: 6% variance
PC1: 62% variance
C
Ins2 (CPM)
0.10
0.05
0.00
Ins2+/+
Ins2-/-
D
Ins2+/+
Ins2-/-
Ccnd1
Ppfia1
Ddx17
Trim30d
A730035I17Rik
Tpcn2
Serpini1
Dtl
Ahcyl
Rps13-ps1
Pdzrn3
Aars
Nxph3
Lxn
Vwc2l
Cenps
Cox16
Rgs4
Gm26793
Row Z-score
-4 -2 0 2 4
E
aerobic respiration
oxidative phosphorylation
ribose phosphate biosynthetic process
purine−containing compound biosynthetic process
nucleoside phosphate biosynthetic process
nucleoside phosphate metabolic process
translation
proton transmembrane transport
purine−containing compound metabolic process
ribose phosphate metabolic process
carbohydrate derivative biosynthetic process
organophosphate biosynthetic process
respiratory electron transport chain
ATP metabolic process
organophosphate metabolic process
ATP synthesis coupled electron transport
mitochondrial respiratory chain complex assembly
carbohydrate derivative metabolic process
organic acid metabolic process
epithelium development
−4 0 4 8
−log10(FDR)
NES
2
1
0
−1
Gene ratio
0.4
0.5
0.6
0.7

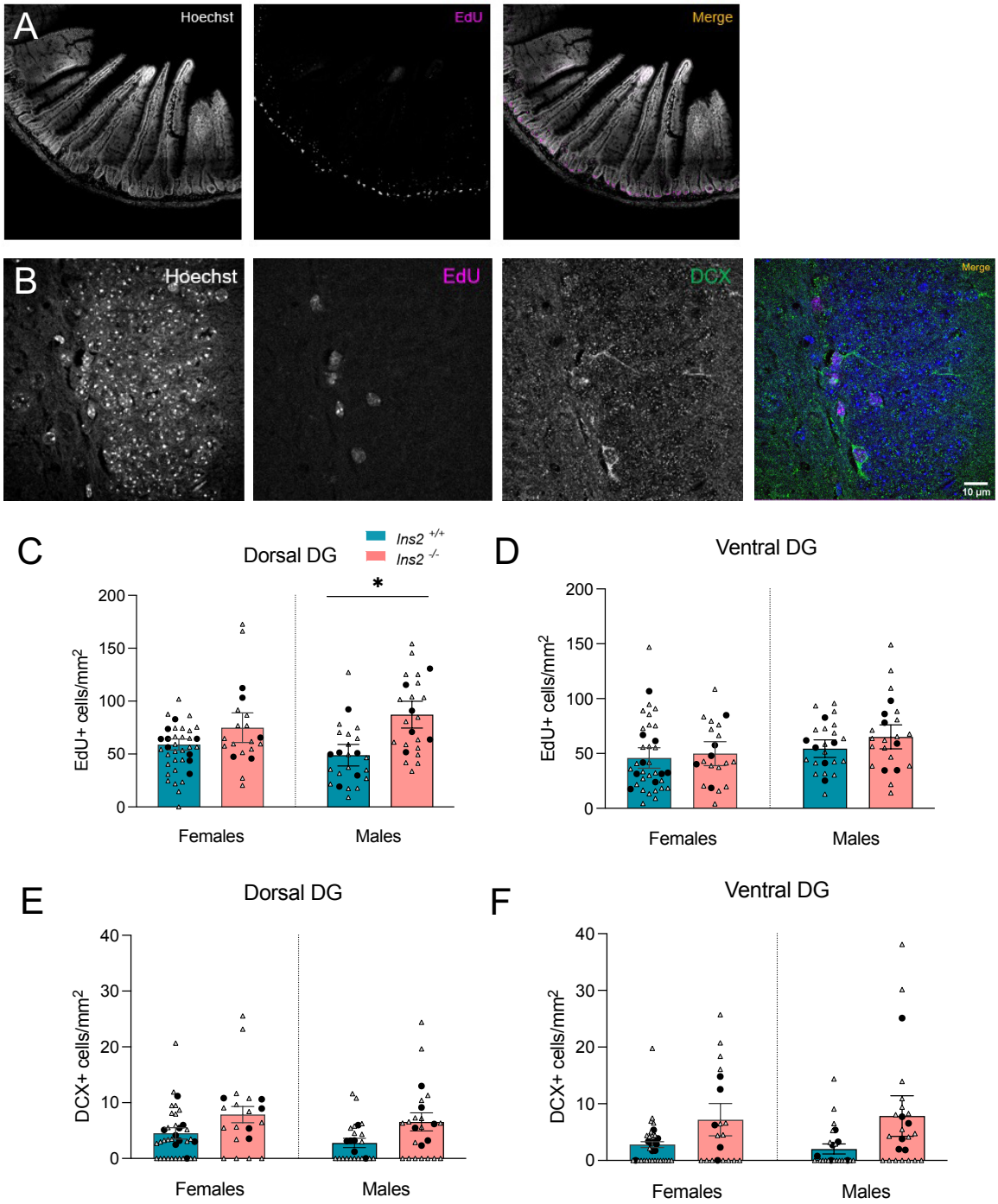
A
Hoechst
EdU
Merge
B
Hoechst
EdU
DCX
Merge
10 µm
C
Dorsal DG
Ins2 +/+
Ins2 -/-
*
EdU+ cells/mm2
200
150
100
50
0
Females
Males
D
Ventral DG
EdU+ cells/mm2
200
150
100
50
0
Females
Males
E
Dorsal DG
DCX+ cells/mm2
40
30
20
10
0
Females
Males
F
Ventral DG
DCX+ cells/mm2
40
30
20
10
0
Females
Males